Inorg. Chem. **2005**, *44*, 6641–6645

Synthesis and Characterization of $Mn_2P_2S_6$ Single-Crystal Nanorods and Nanotubes

Chunhui Li, Xun Wang, Qing Peng, and Yadong Li*

Department of Chemistry and the Key Laboratory of Atomic & Molecular Nanosciences (Ministry of Education, China), Tsinghua University, Beijing 100084, People's Republic of China, and National Center for Nanoscience and Nanotechnology, Beijing 100084, People's Republic of China

Received October 13, 2004

$Mn_2P_2S_6$ single-crystal nanorods with diameters 20–40 nm and lengths up to 1 μm and nanotubes with diameters 40–50 nm and lengths ranging between 110 and 170 nm have been prepared through a low-temperature solvothermal method. They have been characterized by X-ray diffraction, transmission electron microscopy (TEM), high-resolution (HR) TEM, electron diffraction, energy-dispersive spectrometry analysis, X-ray photoelectron spectroscopy, and Raman spectroscopy.

Introduction

The layered compound, transition-metal thiophosphates $M_2P_2S_6$, in which M stands for a divalent transition metal, form a class of layered semiconductors. The structure of $M_2P_2S_6$ is composed of stacking of sulfur-based sandwich layers weakly bonded by van der Waals forces. These lamellar compounds may undergo intercalation/deintercalation reactions involving host−guest redox processes, and the relevant intercalated materials may have many new original properties. Since the 1970s, both the pure and intercalation compounds of $M_2P_2S_6$ layered materials have enjoyed considerable attention because of their basic physical and chemical behavior in terms of their anisotropy[1−3] as well as their potential applications as cathode materials for secondary batteries,[4] ion-exchange applications,[5] ferroelectric materials,[6] and nonlinear optically active materials.[7−9]

Conventionally, $M_2P_2S_6$ compounds are usually synthesized by classical solid-state chemistry processes where elements are mixed in stoichiometric proportions and heated around 700 °C for one to several weeks in an evacuated sealed tube, making the process too long for practical purposes.[10] However, the above-mentioned synthetic route only leads to bulk $M_2P_2S_6$ with a small surface that limits their potential application in gas absorption/separation and catalysis. $M_2P_2S_6$ compounds can be alternatively prepared by coordination of $[P_2S_6]^{4-}$ anions to M^{2+} cations in aqueous solutions or a room-temperature solid-state reaction. The as-prepared products are a nanopartical-agglomerated mass,[11,12] but the reaction yield is lower than that of the ceramic method and the products are usually poor crystalline, even amorphous, which limits their practical applications such as kinetic reversibility and electrical conductivity. Up to now, precise control over phases, sizes, and dimensionalities of the $M_2P_2S_6$ species remains a difficult challenge for materials scientists, which may be critical for the tuning of properties of these novel compounds. Here we will demonstrate a facile solvothermal synthetic route to prepare pure $Mn_2P_2S_6$ with high yields under relatively low temperature conditions, which can be further expanded to the synthesis of other $M_2P_2S_6$ species, and meanwhile by using sodium dodecyl sulfate (SDS) as the structure-directing reagent, uniform $Mn_2P_2S_6$ nanorods and nanotubes could be readily obtained following a formation process characteristic of a rolling mechanism.

* To whom correspondence should be addressed. E-mail: ydli@tsinghua.edu.cn. Fax: (+86) 10-62788765.

(1) Brec, R. *Solid State Ionics* **1986**, *22*, 3−30.
(2) Joy, P. A.; Vasudevan, S. *Phys. Rev. B* **1992**, *46*, 5425−5433.
(3) Grasso, V.; Neri, F.; Patane, S.; Silipigni, L. *Phys. Rev. B* **1990**, *42*, 1690−1695.
(4) Brec, R.; Schleigh, D.; Louisy, A.; Rouxel, J. *Inorg. Chem.* **1979**, *18*, 1814−1818.
(5) Joy, P. A.; Vasudevan, S. *J. Am. Chem. Soc*. **1992**, *114*, 7792−7801.
(6) Simon, A.; Ravez, J.; Maisonneuve, V.; Payen, C.; Cajipe, V. B. *Chem. Mater*. **1994**, *6*, 1575−1580.
(7) Yitzchaik, S.; DiBella, S.; Lundquist, P. M.; Wong, G. K.; Marks, T. J. *J. Am. Chem. Soc*. **1997**, *119*, 2995−3002.
(8) Lacroix, P. G.; Clement, R.; Nakatani, K.; Zyss, J.; Ledoux, I. *Science* **1994**, *236*, 658−660.
(9) Lagadic, I.; Lacroix, P. G.; Clement, R. *Chem. Mater*. **1997**, *9*, 2004−2012.
(10) Taylor, B. E.; Steger, J.; Wold, A. *J. Solid State Chem*. **1973**, *7*, 461−467.
(11) Prouzet, E.; Fukatani, M.; Barj, M.; Janvier, P. *J. Chem. Soc., Dalton Trans*. **1999**, 635−637.
(12) Huang, Z. L.; Zhao, J. T.; Mi, J. X.; Mao, S. Y.; Zheng, L. S. *J. Solid State Chem*. **1999**, *144*, 388−391.

10.1021/ic048570d CCC: $30.25
Published on Web 08/20/2005

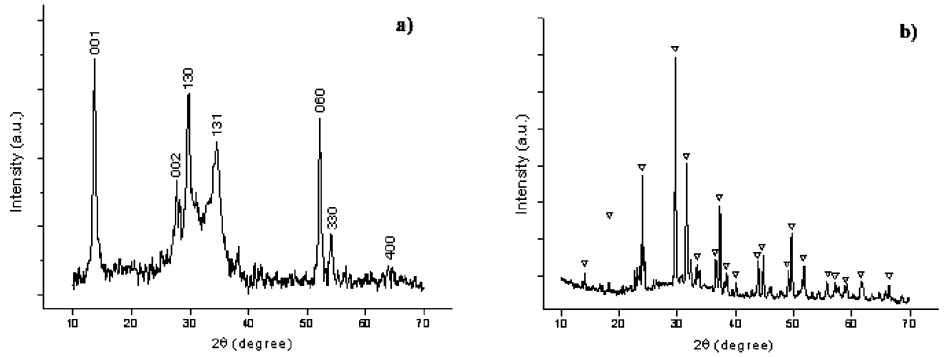

Figure 1. (a) XRD patterns of $Mn_2P_2S_6$. (b) XRD patterns of $Mn_2(PO_4)Cl$.

Experimental Section

Synthesis. Our synthesis is based on a facile ion-exchange solvothermal method. $Na_4P_2S_6$ was prepared according to the literature.[13] The chemical reaction for the synthesis of the $Mn_2P_2S_6$ nanorods/nanotubes can be formulated as

$$2MnCl_2{\cdot}4H_2O + Na_4P_2S_6 \rightarrow Mn_2P_2S_6 + 4NaCl + 8H_2O$$

To prepare $Mn_2P_2S_6$ nanorods, 0.346 g of $Na_4P_2S_6$ (1 mmol) and 0.4 g of $MnCl_2{\cdot}4H_2O$ (2 mmol) were mixed in 15 mL of carbon disulfide. After stirring for several minutes, the mixture was then transferred into a 50-mL autoclave, which was filled up to 80% of the total volume, sealed, and heated at 140 °C for ahout 48 h. (**Caution!** The system should be air-proofed tightly because carbon disulfide is combustible.) The system was then allowed to cool to room temperature. The final product was collected by filtration, washed with deionized water and ethanol to remove any possible ionic remnants, and then dried at 50 °C. To get uniform nanorods/nanotubes products, 0.2 g of SDS was added to the reaction system.

Characterization. Power X-ray diffraction (XRD) was performed on a Bruker D8-Advance X-ray powder diffractometer with Cu Kα radiation (λ = 1.5418 Å). The 2θ range used in the measurement of $Mn_2P_2S_6$ was from 10 to 70° in steps of 0.02°. Transmission electron microscopy (TEM) images were taken with a Hitachi model H-800 transmission electron microscope using an accelerating voltage of 200 kV. The structure and composition of the nanorods were measured by high-resolution TEM (HRTEM; JEOL 2010F). Raman spectra were obtained by using an RM 2000 microscope confocal Raman spectrometer (Renishaw PLC, England) employing a 514-nm laser beam. The composition of the products was also characterized by using a PHI-5300 ESCA X-ray photoelectron spectrometer.

Results and Discussion

As shown in Figure 1a, all of the reflections of the XRD patterns can be readily indexed to a pure monoclinic phase of $Mn_2P_2S_6$ with lattice constants a = 6.077 Å, b = 10.524 Å, c = 6.769 Å, and β = 107.35° (JCPDS No. 78-0495). The 2θ peaks at values of 13.64, 27.48, 29.74, 34.78, 52.10, 54.12, and 64.18° correspond to the crystal planes of [001], [002], [130], [131], [060], [330], and [400] of the crystalline $Mn_2P_2S_6$ species, respectively. The XRD pattern indicates that pure $Mn_2P_2S_6$ can be obtained under the current synthetic conditions. The d value at 34.79° is calculated to be approximately 0.257 nm, corresponding to the [131] plane spacing of the $Mn_2P_2S_6$ species.

Scheme 1

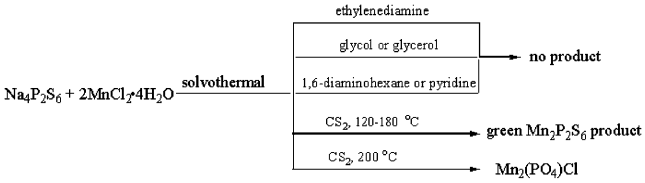

Influence of the Solvents. The influence of the solvents was investigated by several experiments conducted in different solvents. As shown in Scheme 1, when carbon disulfide was used as the reaction medium, pure-phase $Mn_2P_2S_6$ can be obtained. However, when ethylenediamine, glycol, glycerol, 1.6-diaminohexane, and pyridine were used as the solvothermal synthetic solvent, there was no green $Mn_2P_2S_6$ formed among the products. On the basis of the experiments, we believe that these coordinating solvent molecules can form stable complexes with Mn^{2+}, thus reducing the reactivity of Mn^{2+} and preventing the formation of the $Mn_2P_2S_6$ phase.

Influence of the Reaction Temperatures. In our adopted temperature range (100−180 °C), the phase does not change with the temperature, and the crystallinity increases with an increase in the temperature. If the reaction temperature is higher than 200 °C, a white $Mn_2(PO_4)Cl$ is produced (Figure 1a,b), which shows that $Mn_2P_2S_6$ is not stable under those conditions.

Influence of the Surfactants. On the basis of the successful synthesis of $Mn_2P_2S_6$, we have attempted to confine its dimensionalities under similar solvothermal conditions, which have been evidenced to be critical for the tuning of properties of materials in the past decades.[14−18] Because $Mn_2P_2S_6$ species have lamellar structures in nature, similar to those of graphite, bismuth, WS_2, and MoS_2 compounds, it is most probable that they may form nanotubes

(13) Falius, H. *Z. Anorg. Allg. Chem.* **1968**, *356*, 189.

(14) Xia, Y. N.; Yang, P. D.; Sun, Y. G.; Wu, Y. Y.; Mayers, B.; Gates, B.; Yin, Y. D.; Kim, F.; Yan, Y. Q. *Adv. Mater.* **2003**, *15*, 353−389.

(15) Hu, J. Q.; Bando, Y.; Liu, Z. W.; Sekiguchi, T.; Golberg, D.; Zhan, J. H. *J. Am. Chem. Soc.* **2003**, *125*, 11306−11313.

(16) Yang, J.; Liu, Y. C.; Lin, H. M.; Chen, C. C. *Adv. Mater.* **2004**, *16*, 713−716.

(17) (a) Sun, X. H.; Li, C. P.; Wong, W. K.; Wong, N. B.; Lee, C. S.; Lee, S. T.; Teo, B. K. *J. Am. Chem. Soc.* **2002**, *124*, 14464−14471. (b) Liu, C. H.; Zapien, J. A.; Yao, Y.; Meng, X. M.; Lee, C. S.; Fan, S. S.; Lifshitz, Y.; Lee, S. T. *Adv. Mater.* **2003**, *15*, 838−841.

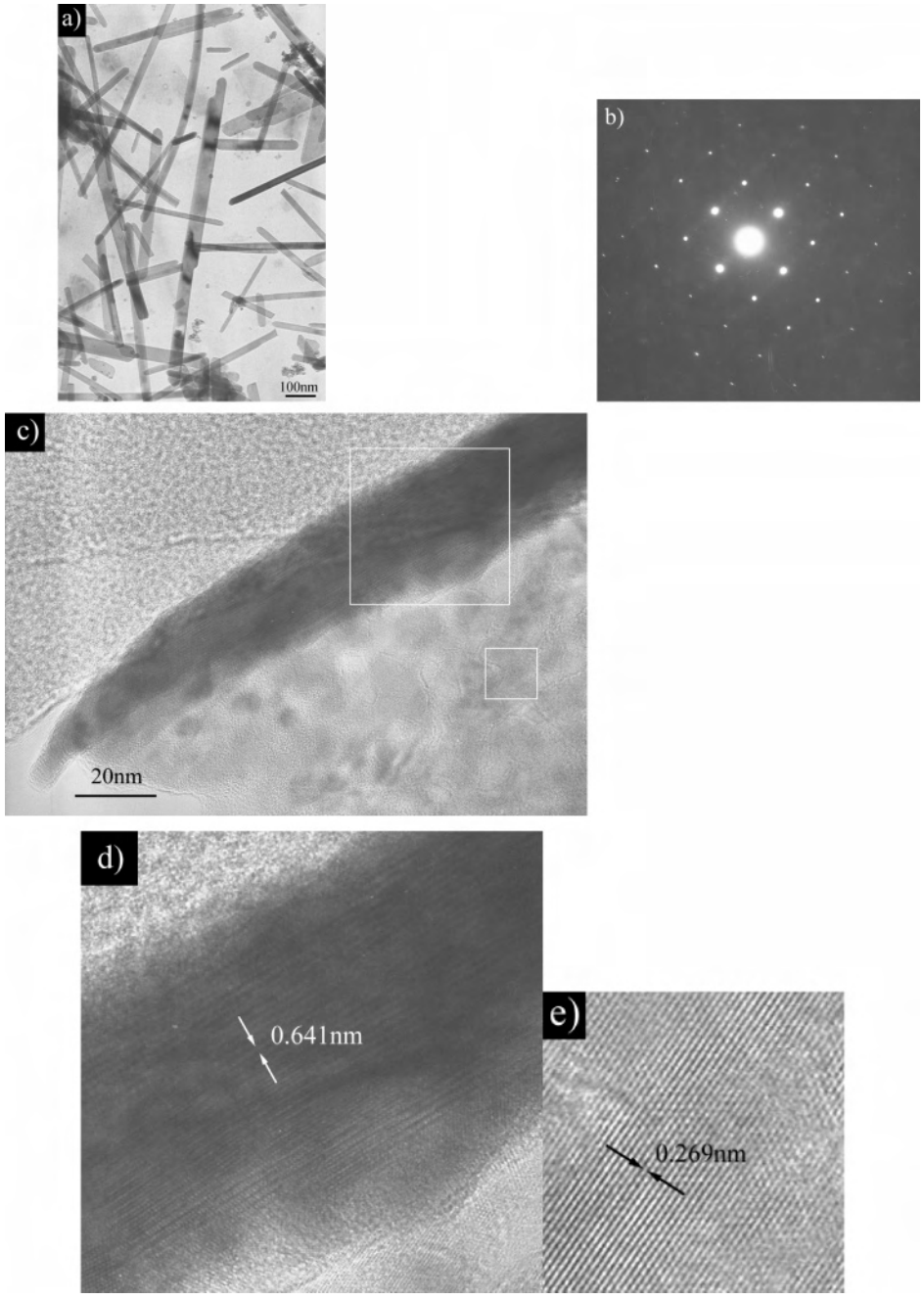

Figure 2. (a) TEM image of $Mn_2P_2S_6$ nanorods. (b) Electron diffraction pattern of a single $Mn_2P_2S_6$ nanorod. (c) HR TEM picture showing the curling at the edge of a $Mn_2P_2S_6$ plate. (d) Magnification of the square section (upper) in part c. (e) Magnification of the square section (below) in part c.

or nanowires under the appropriate conditions, and the key is how to overcome the interactions between layers and provide the driving force for the rolling process.[18−21]

To facilitate this process, different surfactants, such as cetyltrimethylammonium bromide, SDS, poly(vinylpyrrolidone), and poly(vinyl alcohol), have been investigated. Experimental results showed that $Mn_2P_2S_6$ products with regular morphology only could be obtained from the experiment employing SDS as the structure-directing reagent.

As shown in Figure 2a, all of the samples dispersed on the TEM grids show rodlike morphology with diameters of approximately 20−40 nm and lengths ranging between 150 nm and 1 μm. Electron diffraction patterns of $Mn_2P_2S_6$, taken from a single rod, are consistent with the single-crystalline nature of the product (Figure 2b).

(18) (a) Li, Y. D.; Wang, J. W.; Deng, Z. X.; Wu, Y. Y.; Sun, X. M.; Yu, D. P.; Yang, P. D. *J. Am. Chem. Soc.* **2001**, *123*, 9904−9905. (b) Li, Y. D.; Li, X. L.; Deng, Z. X.; Zhou, B. C.; Fan, S. S.; Wang, J. W.; Sun, X. M. *Angew. Chem., Int. Ed.* **2002**, *41*, 333−335. (c) Li, Y. D.; Li, X. L.; He, R. R.; Zhu, J.; Deng, Z. X. *J. Am. Chem. Soc.* **2002**, *124*, 1411−1416. (d) Li, Y. D.; Li, X. L. *Chem. Eur. J.* **2003**, *9*, 2726−2731.

(19) (a) Sun, X. M.; Li, Y. D. *Chem. Eur. J.* **2003**, *9*, 2229−2238. (b) Chen, X.; Sun, X. M.; Li, Y. D. *Inorg. Chem.* **2002**, *41*, 4524−4530. (c) Wang, X.; Li, Y. D. *Chem. Lett.* **2004**, *33*, 48−49.

(20) Wang, X.; Zhuang, J.; Chen, J.; Zhou, K. B.; Li, Y. D. *Angew. Chem., Int. Ed.* **2004**, *43*, 2017−2020.

(21) (a) Li, Y. D.; Liao, H. W.; Ding, Y.; Fan, Y.; Zhang, Y.; Qian, Y. T. *Inorg. Chem.* **1999**, *38*, 1382−1387. (b) Deng, Z. X.; Li, L. B.; Li, Y. D. *Inorg. Chem.* **2003**, *42*, 2331−2341.

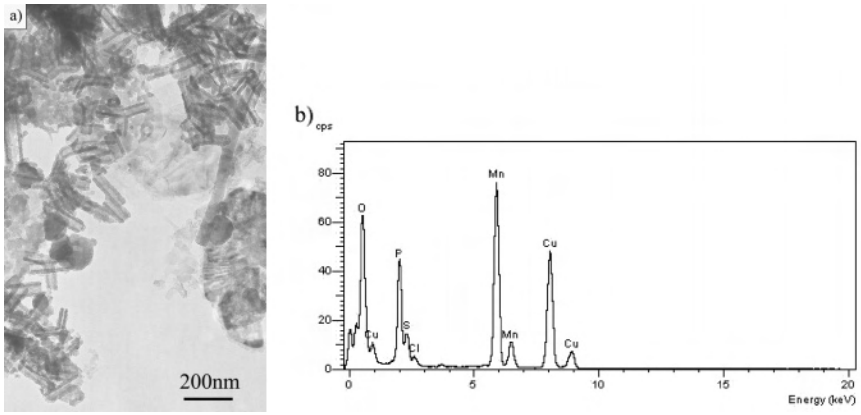

Figure 3. (a) TEM image of $Mn_2P_2S_6$ nanotubes. (b) EDS analysis of nanotubes in part a.

Formation Mechanism Analyses of the Products. To investigate the formation process of these nanorods, the reaction times have been shortened from a routine 48 h to 24 h. Many $Mn_2P_2S_6$ plates with curled edges were found coexisting with the nanorods products. Figure 2c is a typical image. These plates can be considered to be in the initial stage of the rolling process of the molecular layers. HRTEM analysis provides more detailed structural information on the curling intermediates. The interlayer distance of the curling edges is calculated to be approximately 0.641 nm, which corresponds to the separation between [001] planes (Figure 2d) with the biggest plane separations and the interaction between these planes is the weakest; thus, the curling behavior occurred along with the [001] plane. Figure 2e shows the HRTEM image of the central part of the plate, and the interlayer spacing can be calculated to be about 0.269 nm, corresponding to the interlayer spacing of the [131] plane of the $Mn_2P_2S_6$ species. It is apparent that a rolling process has occurred along with the reaction and will be responsible for the formation of the final nanorods.

It is believed that SDS anions can form intermediates with Mn^{2+} ions induced by electrostatic interaction, which is responsible for the formation of $Mn_2P_2S_6$ nanorods. Therefore, it is not difficult to understand that cation surfactants and neutral surfactants show no effect on the morphology of products because of their inability to form coordination intermediates needed for 1D anisotropic growth. In our opinion, the formation of $Mn_2P_2S_6$ nanorods comprised several main steps: (1) The SDS anions condensed into aggregations with Mn^{2+} cations to form lamellar structures. (2) The ion-exchange reaction between $MnCl_2$ and $Na_4P_2S_6$ led to the $Mn_2P_2S_6$ species, while the lamellar structures remained. (3) During treatment under solvothermal conditions, the condensation process continued and brought out more ordered lamellar assemblies. (4) These lamellar sheets began to loosen at the sheet edge and rolled onto themselves to finally form $Mn_2P_2S_6$ nanorods/nanotubes.

$Mn_2P_2S_6$ nanotubes were also observed in the product when the reaction time was shortened. As shown in Figure 3a, the TEM image indicates that the as-synthesized $Mn_2P_2S_6$ nanotubes have uniform outer diameters of 40−50 nm and lengths ranging from 110 to 170 nm. The presence of $Mn_2P_2S_6$ nanotubes further validated the rationality of the rolling mechanism. Energy-dispersive spectrometry (EDS) analysis (Figure 3b) taken from an individual nanotube has indicated that Mn, P, and S are present; the peaks of O and Cl may be attributed to the water molecules and chlorine ions absorbed in the sample.

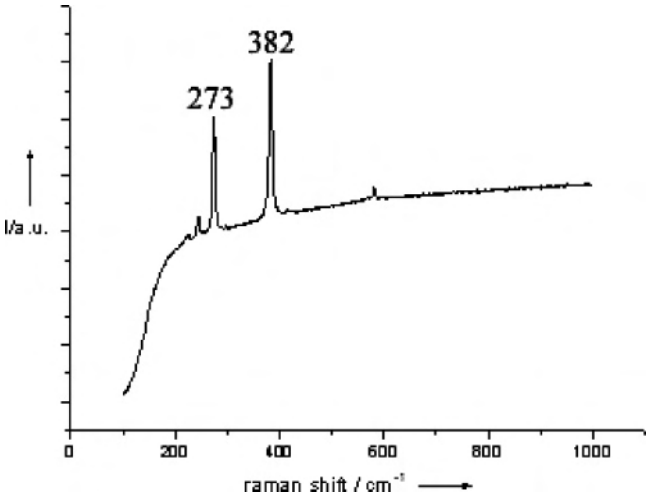

Figure 4. Raman spectra of product obtained when the reaction time was shortened.

Raman and X-ray Photoelectron Spectroscopy (XPS) Spectra. In our experiments, SDS acted as the structure-directing reagent in the formation of $Mn_2P_2S_6$ nanorods/nanotubes, and then it seems reasonable to imagine that SDS may exist in the final products in a way similar to that of vanadium oxide nanotubes.[22] However, our experimental results show that this is not the case. The Raman spectrum was taken from an $Mn_2P_2S_6$ product with a reaction time of 12 h. As shown in Figure 4, only the virbration peaks of $Mn_2P_2S_6$ could be observed, the most intense peak at 382 cm^{-1} could be assigned to the mixed symmetric P−P and P−S stretching modes (A_{1g}), and the strong peak at 273 cm^{-1} could be assigned to the P_2S_6 deformation vibrations (S−P−S and S−P−P modes (E_g)), according to the reported literature,[12] which showed that the products were pure $Mn_2P_2S_6$, without surfactant embedded in them. Considering the corresponding peaks of $Na_4P_2S_6{\cdot}6H_2O$ located at 377 and 261 cm^{-1}, respectively, the shift of the peaks between

(22) Patzke, G. R.; Krumeich, F.; Nesper, R. *Angew. Chem., Int. Ed.* **2002**, *41*, 2446−2461.

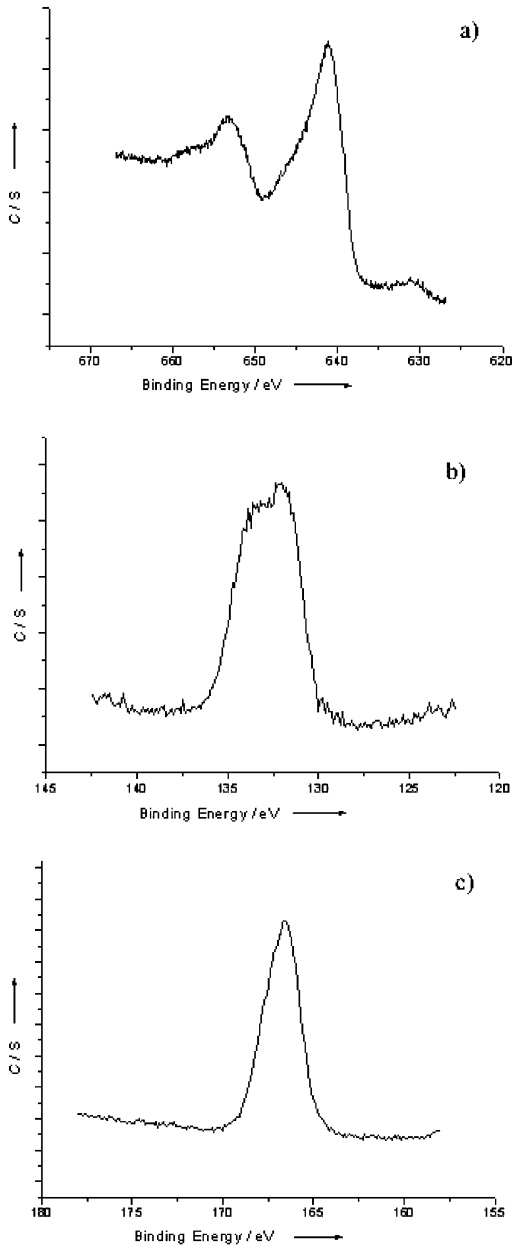

Figure 5. XPS spectra of Mn 2d, P 2p, and S 2p of the $Mn_2P_2S_6$ nanotubes: (a) Mn 2p; (b) P 2p; (c) S 2p.

$Na_4P_2S_6 \cdot 6H_2O$ and $Mn_2P_2S_6$ spectra signifies a change in the structural environment of the $P_2S_6^{4-}$ anion before and after the reaction.

XPS spectra of Mn 2p, P 2p, and S 2p are shown in Figure 5 and correspond to the $Mn_2P_2S_6$ 1D nanotubes. The results obtained in the case of $Mn_2P_2S_6$ nanotubes for Mn 2p, S 2p, and P 2p peaks did not seem to depend on the sizes of the species, with the examples of $Mn_2P_2S_6$ being given in Table 1, and were similar to those observed for bulk $Mn_2P_2S_6$.[23] The systematic shift of about 0.2 eV toward high binding energies is not siginificant and probably is due to a difference calibration scale (C 1s at 284.8 eV for $Mn_2P_2S_6$).

Influence of the Reactant Concentrations. The sizes of these nanorods are flexible to some extent; the reaction time and concentration have been found to be responsible for the size and shape control of these nanostructures. As shown in parts a and b of Figure 6, the diameters of the $Mn_2P_2S_6$ nanorods increase from approximately 20 to 100 nm when the reactant concentration (based on $Na_4P_2S_6$) changed from 0.05 to 0.0125 M. It is generally believed that the higher the concentration of the reactants is, the larger the amount of crystal seeds that are formed at the beginning of the reaction and the shorter the anisotropic growth process is. As is shown in Figure 6a,b, there is an apparent increase in the ratio of length to diameter, from 6−7 to 20−30; thus, it may safely be concluded that the crystal growth process is indeed prolonged with a decrease in the concentration of the reactants.

Table 1. XPS Results for the $Mn_2P_2S_6$ Bulk and $Mn_2P_2S_6$ Nanotubes at the Mn 2p, P 2p, and S 2p Levels[a]

peak	$Mn_2P_2S_6$ bulk	$Mn_2P_2S_6$ nanotubes
Mn $2p_{3/2-1/2}$	641.2−652.8	641.4−653.5
P $2p_{3/2-1/2}$	131.7−132.8	131.9−133.5
S $2p_{3/2-1/2}$	162.2−163.4	162.4

[a] Binding energies are given in electronvolts.

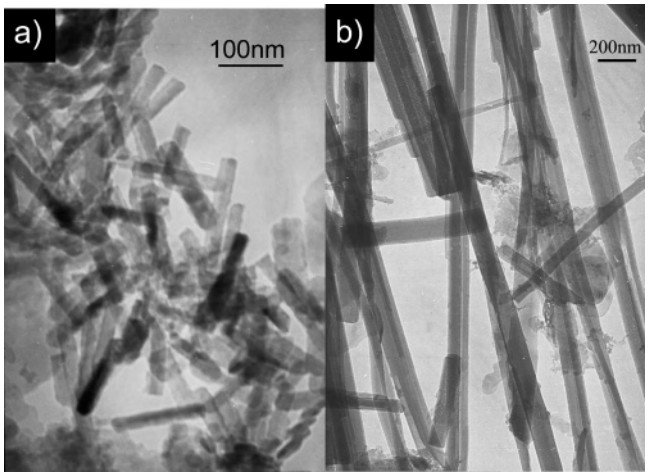

Figure 6. TEM image of $Mn_2P_2S_6$: (a) 0.05 M, 140 °C, 48 h; (b) 0.0125 M, 140 °C, 48 h (concentration based on $Na_4P_2S_6$).

Conclusions

In summary, $Mn_2P_2S_6$ single-crystal nanorods and nanotubes have been successfully prepared based on the "rolling mechanism" via a facile ion-exchange solvothermal process, which overcame the disadvantages of methods reported. We believe that this method can also be extended to the preparation of other $M_2P_2S_6$ 1D nanostructured materials with higher purity and uniformity, and these distinctive structures will expand their applications in optoelectronic and nanoscale devices, nonlinear optics, and magnetic materials.

Acknowledgment. This work was supported by NSFC (Grants 50372030, 20025102, and 20131030), the Specialized Research Fund for the Doctoral Program of Higher Education, the Foundation for the Author of National Excellent Doctoral Dissertation of People's Republic of China, and the State Key Project of Fundamental Research for Nanomaterials and Nanostructures (Grant 2003CB716901).

IC048570D

(23) Gonbeau, D.; Coradin, T.; Clement, R. *J. Phys. Chem. B* **1999**, *103*, 3545−3551.